



**HAL**  
open science

## The human Vps29 retromer component is a metallo-phosphoesterase for a cation-independent mannose 6-phosphate receptor substrate peptide

Ester Damen, Elmar Krieger, Jens Nielsen, Jelle Eygensteyn, Jeroen E M van Leeuwen

### ► To cite this version:

Ester Damen, Elmar Krieger, Jens Nielsen, Jelle Eygensteyn, Jeroen E M van Leeuwen. The human Vps29 retromer component is a metallo-phosphoesterase for a cation-independent mannose 6-phosphate receptor substrate peptide. *Biochemical Journal*, 2006, 398 (3), pp.399-409. 10.1042/BJ20060033 . hal-00478506

**HAL Id: hal-00478506**

**<https://hal.science/hal-00478506>**

Submitted on 30 Apr 2010

**HAL** is a multi-disciplinary open access archive for the deposit and dissemination of scientific research documents, whether they are published or not. The documents may come from teaching and research institutions in France or abroad, or from public or private research centers.

L'archive ouverte pluridisciplinaire **HAL**, est destinée au dépôt et à la diffusion de documents scientifiques de niveau recherche, publiés ou non, émanant des établissements d'enseignement et de recherche français ou étrangers, des laboratoires publics ou privés.

## The human Vps29 retromer component is a metallo-phosphoesterase for a cation-independent mannose 6-phosphate receptor substrate peptide

Ester DAMEN\*, Elmar KRIEGER†, Jens E. NIELSEN‡, Jelle EYGENSTEYN§ and Jeroen E.M. van LEEUWEN\*<sup>1</sup>

\*Department of Cell Biology, †Centre for Molecular and Biomolecular Informatics, §Department of General Instrumentation, Faculty of Sciences, Radboud University Nijmegen, Toernooiveld 1, 6525 ED Nijmegen, The Netherlands, ‡Centre for Synthesis and Chemical Biology, School of Biomolecular and Biomedical Science, University College Dublin, Belfield, Dublin 4, Ireland

The retromer complex is involved in the retrograde transport of the cation-independent mannose 6-phosphate receptor (CI-M6PR) from endosomes to the Golgi. It is a heterotrimeric complex composed of Vps26, Vps29 and Vps35 proteins, which are conserved in eukaryote evolution. Recently, elucidation of the crystal structure of Vps29 revealed that Vps29 contains a metallo-phosphoesterase fold [Wang, Guo, Liang, Fan, Zhu, Zang, Zhu, Li, Teng, Niu, Dong, and Liu (2005) *J. Biol. Chem.* **280**, 22962-22967; Collins, Skinner, Watson, Seaman and Owen (2005) *Nat. Struct. Mol. Biol.* **12**, 594-602]. We demonstrate that recombinant human (h)Vps29 displays *in vitro* phosphatase activity towards a serine phosphorylated peptide, containing the acidic-cluster dileucine motif of the cytoplasmic tail of the CI-M6PR. Efficient dephosphorylation required the additional presence of recombinant hVps26 and hVps35 proteins, which interact with hVps29. Phosphatase activity of hVps29 was greatly reduced by alanine substitutions of active site residues that

are predicted to coordinate metal ions. Using inductively coupled plasma mass spectrometry we demonstrate that recombinant hVps29 binds zinc. Moreover, hVps29-dependent phosphatase activity is greatly reduced by a-specific and zinc-specific metal ion chelators, which can be completely restored by addition of excess ZnCl<sub>2</sub>. The binuclear Zn<sup>2+</sup> centre and phosphate group were modelled into the hVps29 catalytic site and pKa calculations provided further insight into the molecular mechanisms of Vps29 phosphatase activity. We conclude that the retromer complex displays Vps29-dependent *in vitro* phosphatase activity towards a serine phosphorylated acidic-cluster dileucine motif that is involved in endosomal trafficking of the CI-M6PR. The potential significance of these findings with respect to regulation transport of cycling TGN proteins is discussed.

Key words: Vps29, Retromer, cation-independent mannose 6-phosphate receptor (CI-M6PR), metallo-phosphoesterase, zinc-binding protein.

Abbreviations used: A-ALP, alkaline phosphatase; CI-M6PR, cation-independent mannose 6-phosphate receptor; CPY, carboxy-peptidase Y; DPAP A, dipeptidyl aminopeptidase A; GGA, Golgi-localizing, gamma-adaptin ear domain homology, ARF-binding; SNX, sorting nexin; PACS-1 phosphofurin cluster sorting protein-1; TGN trans-Golgi network; TIP47, tail-interacting protein of 47 kD); VHS, Vps27, Hrs and Stam; Vps, vacuolar sorting proteins.

<sup>1</sup>To whom correspondence should be addressed (email: J.vanLeeuwen@science.ru.nl).

## INTRODUCTION

Eukaryotic cells contain several membrane-enclosed compartments (organelles), each of which has a unique function that is maintained by correct localisation and retention of its resident proteins. Eukaryote subcellular organization therefore requires the existence of specific protein sorting and transport pathways to and between various organelles. Genetic screens in *Saccharomyces cerevisiae* have identified several Vps (vacuolar sorting proteins) genes whose products are involved, directly or indirectly, in anterograde or retrograde transport between the Golgi and the lysosome-like vacuole [1-3]. Five of those gene products form the retromer complex in yeast; Vps26, Vps29, Vps35, Vps5 and Vps17, which co-localize on early endosomes [4-6] and are involved in retrograde endosome-to-Golgi transport [7].

In yeast, the Vps35 subunit interacts with the cargo protein Vps10p, which is a type I transmembrane receptor that is involved in the sorting of newly synthesized soluble vacuolar hydrolases, such as carboxy-peptidase Y (CPY), from the trans-Golgi network (TGN) to the prevacuolar compartment. In the acidic environment, CPY dissociates from Vps10p and is then transported to the vacuole [8-10]. In contrast, Vps10p is recognized by the Vps35 subunit of the retromer complex, which

functions in the retrograde transport of Vps10p from the pre-vacuolar compartment back to the TGN [11]. In the TGN, Vps10 can carry out additional rounds of enzyme delivery [9, 10].

Orthologs of the yeast retromer proteins appear to be conserved in nearly all eukaryotes, including mammals. Given the role of the retromer complex in yeast, it is likely that the mammalian retromer functions in transport between the endosomes and the TGN. Although yeast protein Vps10p does not have an ortholog in mammals, mannose 6-phosphate receptors (M6PRs) function in an essentially similar manner. Indeed, retromer subunits co-localize with the cation-independent M6PR (CI-M6PR) cargo protein [4, 6] and hVps35 directly interacts with the CI-M6PR in the prelysosomal compartment [4]. The CI-M6PR is involved in the sorting and transport of newly synthesized lysosomal hydrolases that contain mannose 6-phosphate moieties on their N-glycan chains, which serve as sorting signals for TGN-to-endosome transport [12]. One of the triggers of this anterograde transport is the phosphorylation of Ser-2492 in the cytoplasmic tail of the CI-M6PR [13]. This serine is part of the acidic-cluster dileucine sequence DDSDEDLLHI, present in the C-terminus of the CI-M6PR. GGA (Golgi-localizing, gamma-adaptin ear domain

homology, ARF-binding) proteins, which constitute a family of clathrin coat adaptor proteins [14-18], bind with their so-called VHS (Vps27, Hrs and Stam) domain to these acidic-cluster dileucine sorting signals. GGA proteins transport the CI-M6PR, in clathrin coated vesicles, from the TGN to an endosomal compartment *en route* to lysosomes [19-21]. Mutational analysis reveals that Ser-2492 itself is likely to play a role in GGA binding [22] and GST pull-down assays have demonstrated that phosphorylation of this serine increases the affinity of the CI-M6PR for the VHS domains of GGA1 and GGA3 [23].

In the endosomal compartment, the CI-M6PR is able to bind hVps35 [4]. hVps35 is not only the cargo recognition component, but also the scaffold protein of the retromer complex, interacting directly with hVps26 and hVps29 [5, 24]. So far, the role of Vps29 and Vps26 is less clear; Vps29p probably assists Vps35p in cargo binding and Vps26p promotes the interaction between Vps35p and the sorting nexins Vps5p/Vps17p [25]. Vps5p binds with its C-terminal domain to Vps17p to form a dimer [26] which is able to form oligomeric structures, due to the self-assembly activity of Vps5p [7, 27]. This dimer is likely to have a structural role in vesicle budding. In mammals the Vps5p/Vps17p dimer is replaced by its ortholog sorting nexin (SNX) 1 and probably another SNX protein [24]. In the case of the CI-M6PR the cooperation of all components of the retromer complex results in the retrograde transport of the receptor from the endosome to the TGN, where it can continue the transport of hydrolases [4, 6].

Recently, two crystal structures of mammalian Vps29 have been published [5, 28], which revealed that Vps29 contains a metallo-phosphoesterase fold. Metallo-phosphoesterases are enzymes involved in the hydrolysis of phosphate esters [29] that contain two metal ions in their active site. In this study we analyze the function of Vps29 in more detail. Here, we tested the hypothesis that hVps29 acts as a metallo-phosphoesterase for the CI-M6PR. We demonstrate that hVps29 is a zinc-binding protein that acts *in vitro* as a phosphatase on a synthetic phosphopeptide sequence, which is based on the serine phosphorylated C-terminus of the CI-M6PR.

## MATERIALS AND METHODS

### Constructs

hVps29 catalytic site point mutants were constructed by PCR, using the pCIneo hVps29 mammalian expression vector (kindly provided by C.R. Haft, National Institutes of Health, Bethesda, Maryland) as a template. For the hVps29 D8A mutation the following forward and reverse primers (5'-to-3') were used: CCACTTTGCCTTTCTCTCCA and GTTGCACCGGTGTGGGATGTGCAGAGCTCCTAATACCAA. The PCR product was sub-cloned using *EcoRI* and *AgeI* sites. For all other mutations a two-step PCR strategy was used with the following forward and reverse primers: CCACTTTGCCTTTCTCTCCA and ACTGCATTCTAGTTGTGGTT and in addition, for hVps29 N39(A/N) ATTCTCTGCACAGGAG(C/A)TCTTTGCACC AAAGAG and

CTCTTTGGTGCAAAGA(G/T)CTCCTGTGCA  
 GAGAAT; for hVps29 D62(A/N)  
 CATATTGTGAGAGG(CGC/AAA)CTTCGAT  
 GAGAATCTG and  
 CAGATTCTCATCGAAG(GCG/CGC)CCTCT  
 CACAATATG; for hVps29 H86A  
 AAAATTGGTCTGATCGCTGGACATCAAGT  
 TAT and  
 ATAACTTGATGTCCAGCCATCAGACCAAT  
 TTT; for hVps29 H117A  
 ATCTCGGGACACACAGCCAAATTTGAAG  
 CATT and  
 AATGCTTCAAATTTGGCTGTGTGTCCTGA  
 GAT. PCR products were sub-cloned using  
*EcoRI* and *NotI* sites. All mutations were verified  
 by sequencing.

YFP and GST fusion constructs of the  
 retromer subunits were constructed using the  
 pEYFP-C1 vector (Clontech) or pGEX4T1/3  
 vector (Amersham Biosciences). For hVps26,  
 the N-terminal Myc-tag in the pCIneo Myc  
 hVps26 expression construct was replaced by a  
 unique *EcoRI* cloning site followed by an  
 initiation codon, and the C-terminal *EcoRI* site  
 was replaced by a unique *NotI* restriction site.  
 For hVps29, a unique *EcoRI* cloning site was  
 introduced at the 5' end of the pCIneo hVps29  
 Myc cDNA, while the C-terminal Myc-tag was  
 replaced by a stop codon and a unique *NotI*  
 cloning site. The hVps26 and hVps29 cDNAs  
 were cloned in frame into pEYFP-C1 and  
 pGEX4T3 using *EcoRI* and *NotI/Bsp120I*  
 enzymes. For hVps35, the Myc-tag was removed  
 from the pCIneo Myc hVps35 construct and the  
 hVps35 cDNA was cloned in frame into the  
 pEYFP-C1 and pGEX4T1 vector using *XhoI* and  
*NotI/Bsp120I* enzymes.

MycHis fusion constructs of hVps26,  
 hVps29 and hVps35 were constructed by  
 introducing a *KpnI* restriction site before the  
 GST cDNA of the pGEX vectors and replacing  
 the GST coding sequence by a myc-His coding  
 sequence using linked primers.

### Production of GST fusion proteins

GST fusion proteins were produced in the  
*Escherichia coli* XL-2 blue strain containing the  
 appropriate pGEX plasmid. Cultures (0.5–5.0 L)  
 were grown to log phase (OD<sub>600</sub> of 0.6–0.8) and  
 protein expression was induced by addition of  
 isopropyl-1-thio-β-D-galactopyranoside  
 (Invitrogen) to 0.1 mM final concentration. After  
 1–3 h of induction, cells were harvested, rinsed  
 with Tris-buffered saline (TBS) pH 7.4, and  
 resuspended in TBS containing 1% Triton X-  
 100, 100 μg/ml lysozyme and 10 μg/ml each of  
 leupeptin, pepstatin, and aprotinin. The  
 suspension was frozen at –20 °C for at least 16  
 hrs and subsequently thawed at 42 °C followed  
 by sonication. Lysates were cleared by  
 centrifugation for 15 min at 12,000 x g and then  
 incubated with 0.5–3 ml of a 50% slurry of  
 glutathione-Sepharose beads (Sigma) for 2–4 h  
 at 4 °C with rotation. The glutathione-Sepharose  
 beads were washed four times with TBS pH 7.4.

### Production of mycHis fusion proteins

MycHis fusion proteins were produced in the  
*Escherichia coli* XL-2 blue strain containing the  
 appropriate mycHis plasmid. Cultures of 200 ml  
 were grown to log phase (OD<sub>600</sub> of 0.6–0.8) and  
 protein expression was induced by addition of  
 isopropyl-1-thio-β-D-galactopyranoside  
 (Invitrogen) to 0.1 mM final concentration. After

4-5 h of induction, cells were frozen at  $-20\text{ }^{\circ}\text{C}$  for 16 hrs. Cells were thawed on ice and resuspended in 4 ml lysisbuffer (10 mM imidazole, 150 mM NaCl, 50 mM Tris·Cl, pH 8.0) and lysozyme was added to a final concentration of 1 mM. The lysates were sonicated and cleared by centrifugation for 15 min at  $12,000 \times g$ . Cleared lysates were incubated with 1 ml Ni-NTA beads (Qiagen) for 2-3 h at  $4\text{ }^{\circ}\text{C}$  with rotation. The Ni-NTA beads were washed three times (10 mM imidazole, 300 mM NaCl, 50 mM Tris·Cl, pH 8.0) and subsequently eluted with elutionbuffer (250 mM imidazole, 300 mM NaCl, 50 mM Tris·Cl, pH 8.0) and dialysed against  $\text{H}_2\text{O}$ .

### **Pull Down Assays**

NIH3T3 cells were cultured on dishes coated with 0.1% gelatin and grown at  $37\text{ }^{\circ}\text{C}$  in Dulbecco's modified Eagle's medium (DMEM) supplemented with 10% newborn calf serum. pEYFP-C1 vector, Vps26, Vps29 and Vps35 YFP fusion constructs were transiently transfected into NIH3T3 cells using lipofectamin (Invitrogen) according to the manufacturer's instructions. After 22-24 h of transfection, the cells were lysed in lysis buffer (150 mM NaCl, 25 mM Tris pH 7.5, 5 mM EDTA pH 8.0, 1 mM  $\text{Na}_3\text{VO}_4$ , 1 mM NaF, 1 mM phenylmethylsulfonyl fluoride, 1  $\mu\text{g}/\text{ml}$  leupeptin, 1  $\mu\text{g}/\text{ml}$  aprotinin, 1  $\mu\text{g}/\text{ml}$  pepstatin) and the lysates were transferred to Eppendorf tubes and centrifuged for 10 min at  $4\text{ }^{\circ}\text{C}$  at  $13,000 \times g$  in an Eppendorf centrifuge to remove nuclei and cell debris. The cleared lysates were added to purified GST-fusion proteins of hVps26, hVps29, hVps35 or to GST alone that

were bound to GSH agarose beads and incubated for at least 2 h at  $4\text{ }^{\circ}\text{C}$ . Unbound proteins were then removed by washing two times with lysis buffer and once with phosphate-buffered saline.

In case of the pull down experiments with the mycHis fusion proteins, mycHis-tagged hVps29 and hVps35 were purified on Ni-NTA beads, eluted and incubated for at least 2 h at  $4\text{ }^{\circ}\text{C}$  in the presence of hVps26-GST immobilized on GSH agarose beads. Unbound proteins were then removed by washing three times with TBS. Samples were then subjected to *in vitro* phosphatase assays or Western blot analysis.

For Western blot analysis, the nitrocellulose membranes were blocked with 5% bovine serum albumin, incubated with  $\alpha$ -GFP antibody or  $\alpha$ -c-myc(9E10) antibody (Santa Cruz), incubated with appropriate peroxidase-linked secondary antibodies and the immunocomplexes were visualized with enhanced chemiluminescence.

### **In vitro phosphatase assays**

For *in vitro* phosphatase assays on GST fusion proteins alone, GST fusion proteins were separated from their GST tags by incubating the proteins with 10 units of thrombin (Amersham Biosciences) in TBS pH 7.4 in a total volume of 100  $\mu\text{l}$  for at least 16 h. To each sample, 55  $\mu\text{g}$  (1.1 mg/ml) serine phosphorylated peptide SFHDDpSDEDLLHI (>95% purity, Sigma Genosys) and 100  $\mu\text{l}$  Ser/Thr Assay Buffer (50 mM Tris·Cl pH 7.0, 100  $\mu\text{M}$   $\text{CaCl}_2$ ) (Upstate) were added. The proteins were incubated with the phosphopeptide at  $37\text{ }^{\circ}\text{C}$  for 30 min or 16 hrs. From each sample 35  $\mu\text{l}$  were added to 100  $\mu\text{l}$  Biomol Green (Biomol) in a 96-wells dish

(Nunc). To analyze the amount of free phosphate,  $OD_{630\text{ nm}}$  was measured with a Wallac Multilabel counter 1420.

In case of the metal ion chelator experiment, GST fusion proteins were incubated with 5 mM EDTA, EGTA or TPEN (N,N,N',N'-tetrakis(-2-pyridylmethyl)-ethylene-diamine) (Molecular Probes) for 15 min and washed 3 times with TBS prior to thrombin cleavage. For the experiments in the presence of zinc and for the experiments using mycHis constructs,  $ZnCl_2$  was added to the Ser/Thr Assay Buffer at a final concentration of 1 mM.

The volume of the remaining supernatant of the samples was reduced by means of a speed vac concentrator, subjected to SDS-PAGE and proteins were visualized using Coomassie blue staining according to standard procedures.

### **Inductively coupled plasma mass spectrometry**

GST alone and hVps29 GST-fusion proteins were eluted from glutathione-Sepharose beads by incubation with 5 mM reduced glutathione in 50 mM Tris·Cl pH 8.0. The amount of protein in the supernatant was measured using Bio-Rad Protein Assay Dye Reagent Concentrate (Biorad). A small amount of the samples was subjected to SDS-PAGE and proteins were visualized using Coomassie blue staining to confirm expression of the protein. In order to perform accurate measurements, mg quantities of protein should be analyzed. Series of equal amounts of GST alone and hVps29-GST molecules were prepared by dilution with 5 mM reduced glutathione in 50 mM Tris·Cl pH 8.0.  $HNO_3$  was added to a final concentration of 2 M to destroy the proteins. The

final volume of the samples was 5 ml. Samples were centrifuged for 30 min at 5,000 x g and the supernatant was analyzed by ICP-MS (X Series ICP-MS) (Thermo Electron Corporation) controlled with PlasmaLab software v.2.3.0 according to manufacturer's instructions. The measured amount of Mg, Ca, Cr, Fe, Mn, Ni, Co, Cu and Zn metal ions in the samples was quantified in parts per billion (ppb) using dilution series of CentiPur standard solutions (Merck). The number of measured metal molecules was determined using atomic mass numbers (zinc:  $65.37\text{ g}\cdot\text{mol}^{-1}$ ) and a ratio between protein molecules and metal molecules was calculated.

### **Molecular modelling**

Molecular modelling of the hVps29 active site was done with YASARA ([www.yasara.org](http://www.yasara.org)) starting from the crystal structure with two bound  $Mn^{2+}$  ions (PDB ID 1Z2W, [5]). The highly similar structure of the human Ser/Thr protein phosphatase 5 [30] containing two  $Mn^{2+}$  ions plus a bound phosphate was structurally aligned using the SHEBA plugin [31], and subsequently the phosphate coordinates were transferred to Vps29. The  $Mn^{2+}$  ions were replaced by  $Zn^{2+}$  ions to match our experimental findings. The phosphate was modelled as a mono-anion with one hydrogen on O4 (the leaving group) and one on O2, stabilized by the interaction with Asp-62. The bridging water molecule was turned into a hydroxide ion. Finally the protein side chains were energy minimized with the Yamber2 force field to accommodate the changes [32].

### **pKa calculations**

pKa calculations were carried out using the WHAT IF pKa (WIpKa) calculation package as described earlier [33] with the modification that the protein was described by a single dielectric constant of 8. WIpKa relies on DelPhi II [34] to solve the linear form of the Poisson-Boltzmann equation (PBE). The remaining PBE parameters were set as follows: probe radius 1.4 Å; solvent dielectric: 80; final grid resolution 0.25 Å/grd point. Charges and radii were assigned using the OPLS force field [35].

## **RESULTS**

### **Retromer complex performs phosphoesterase activity on a CI-M6PR based substrate**

Vesicular transport between various membrane-enclosed compartments is a fundamental characteristic of all eukaryotes. Most proteins involved in fundamental vesicular trafficking processes are evolutionary conserved. Indeed, phylogenetic analysis (Figure S1 and S2, supplementary material) demonstrates that Vps29 is found in nearly all eukaryotes, including higher eukaryotes (metazoans, plants, fungi) as well as protozoan groups such as diplomonadida, apicomplexa, entamoebidae and kinetoplastidae. Interestingly, BLAST searches also reveal similarity of eukaryote Vps29 proteins to hypothetical archaeal proteins with (putative) phosphoesterase activity (e.g. MJ0936), even though archaea do not contain organelles. Vps29 shows extremely high sequence conservation among vertebrates; only 14 out of the 182 amino acids show sequence

variations, most of which are conservative substitutions (Figure S3, supplementary material).

Recent crystallographic studies demonstrate that Vps29 belongs to the PPP family of calcineurin-like metallo-phosphatases, although Vps29 enzymatic activity has yet to be established [5, 28]. This family is not only found in eukaryotes, but also in archaea and prokaryotes [36]. The crystal structures of members of this family are characterized by a double  $\beta$ -sandwich, surrounded by  $\alpha$ -helices (reviewed in [37]). Metallo-phosphoesterases contain two metal ions in their catalytic site, which stabilize a highly reactive hydroxyl ion at physiological pH that is in position for nucleophilic attack of the phosphoester bond. The positively charged metal ions can also serve as an electrophilic catalyst and stabilize developing negative charge(s) of the metal- $\text{PO}_4$  transition state. The oxy-anion of the substrate leaving group is usually protonated by a catalytic histidine that forms a catalytic dyad with a neighbouring aspartic acid, which provides the histidine with acidic properties. Efficient regeneration of catalytic hydroxyl ions is required for the active status of the enzyme, which has been proposed to occur through a network of hydrogen bonded water molecules in the active site, leading to protonation of a surrounding basic histidine residue and release of the proton into bulk solvent [29].

The metal coordinating and catalytically important residues, mostly aspartates and histidines, are conserved among metallo-phosphoesterase family members and are located within five conserved motifs (I through V)



(Figure S3, supplementary material) in loops connecting the core  $\alpha$  and  $\beta$  secondary structure elements, i.e. DXH(X)<sub>-25</sub> GDXXD(X)<sub>-25</sub> GNH[D/E] (motifs I to III [38, 39]) and GH(X)<sub>-50</sub> GHX[H/X] (motifs IV to V [40]). The corresponding motifs of hVps29 start with Asp-8, Gly-38, Gly-61, Gly-87 and Gly-114, respectively (Figure S3, supplementary material). Interestingly, hVps29 shows three unique features that distinguish hVps29 from other metallo-phosphoesterases with a known crystal structure (Figure S3, supplementary material). First, an aspartic acid is normally found on the position of Asn-39 (motif II). Second, an asparagine is normally found on the position of Asp-62 (motif III). Third, the catalytic histidine (motif III), which serves as a proton donor for the leaving group, is replaced by Phe-63.

In order to determine whether the retromer complex contains phosphatase activity, we first assessed whether the retromer subunits interact using *in vitro* affinity precipitations (Figure 1A). Mammalian expressed YFP fusion proteins (Figure 1B) were incubated with GST-fusion proteins of hVps26, hVps29 and hVps35 (Figure 1C). As seen in Figure 1A, hVps26-GST and hVps35-GST interact with Vps29-YFP but not with YFP alone. Vice versa, hVps29-GST interacts with hVps26-YFP as well as with hVps35-YFP and not with YFP alone. Thus, consistent with earlier reports [5] interaction between retromer subunits can be demonstrated by *in vitro* affinity precipitation.

To determine whether hVps29 is an active metallo-phosphoesterase, we assayed recombinant hVps29 for *in vitro* phosphatase

activity. GST-fusion proteins of hVps26, hVps29 and hVps35 were separately produced in *E. coli* and the respective recombinant proteins were separated from their GST tags using the thrombin cleavage site (Figure 2A). Given that (i) the mammalian retromer complex functions in the retrograde transport of cycling TGN proteins, (ii) retromer subunits co-localize with the CI-M6PR and that (iii) mammalian Vps35 directly interacts with the CI-M6PR in the prelysosomal compartment [4, 6], we used the serine phosphorylated peptide SFHDDpSDEDLLHI, containing the acidic-cluster dileucine motif of the CI-M6PR C-terminal tail, as an *in vitro* phosphatase substrate. Recombinant hVps26, hVps29, hVps35 or a mixture of non-stoichiometric amounts of all three proteins was incubated with the phospho-peptide at 37 °C. The amount of free phosphate, which correlates with the phosphatase activity, was measured in each sample after 30 min and after 16 hrs. Figure 2B shows that there was no dephosphorylation activity detectable after 30 min for the individual retromer proteins. Interestingly, only hVps29 showed phosphatase activity on its own after 16 hrs of incubation. The detected amount of free phosphate was considerably higher than the amount of free phosphate measured in the vector control, or measured in hVps26 and hVps35. Importantly, when the three retromer subunits were added simultaneously to the phosphatase reaction, the phosphatase activity was already detectable after 30 min of incubation. Protein expression in the phosphatase reaction was confirmed by Coomassie brilliant blue staining of the remaining supernatant of the samples used in the assay (Figure 2C).

To further confirm phosphatase activity of the retromer subunits as a complex, we used GST-Vps26 or GST alone coupled to GSH-agarose beads as an affinity matrix for recombinant mycHis-tagged Vps29 and Vps35 proteins that were purified by metal chelation affinity chromatography (MCAC) from bacterial lysates. Consistent with the results shown in Figure 1, both mycHis-tagged Vps29 and Vps35 were detected by anti-Myc Western blotting in GST Vps26 affinity precipitates (Figure 3A), indicating that retromer subunits were able to form a complex *in vitro*. To determine whether these complexes contained phosphatase activity, the GST-Vps26 affinity precipitates containing mycHis-tagged Vps29 and Vps35 were used for an *in vitro* phosphatase assay using the serine phosphorylated SFHDDpSDEDLLHI peptide as a substrate (Figure 3B). Protein expression in the phosphatase assay was confirmed by Coomassie blue staining of the remaining supernatant of the samples used in the assay (Figure 3C). As shown in Figure 3B, affinity precipitates of GST-Vps26 but not GST alone contained phosphatase activity towards the CI-M6PR substrate peptide. The amount of phosphatase activity detected in the GST-Vps26 affinity precipitates was consistently much lower than observed when phosphatase activity was assayed on a mixture of GSH-agarose bound GST-Vps26, -Vps29 and -Vps35 protein following thrombin cleavage (3<sup>rd</sup> bar). It is likely that the reduced phosphatase activity detected in the GST-Vps26 affinity precipitates is due to the presence of reduced amounts of mycHis-tagged Vps29 and Vps35 proteins, since we were unable to detect mycHis-tagged Vps29 and Vps35 in GST-Vps26 affinity

precipitates by Coomassie blue staining (Figure 3C).

Collectively, the data shown in Figure 1-3 demonstrate that (i) Vps26, Vps29 and Vps35 can co-precipitate *in vitro*, (ii) Vps29 alone but not Vps26 or Vps35 contains phosphatase activity, (iii) Vps29 phosphatase activity is greatly enhanced by the additional presence of Vps26 and Vps35 retromer subunits, and (iv) GST-Vps26 affinity matrices acquire phosphatase activity following affinity precipitation of - and complex formation with - mycHis-tagged Vps29 and Vps35 retromer subunits. We conclude that the retromer complex contains *in vitro* phosphatase activity towards the serine phosphorylated peptide SFHDDpSDEDLLHI, containing the acidic cluster dileucine motif of the CI-M6PR cytoplasmic tail.

### Catalytic site mutations of hVps29 inhibit its phosphoesterase activity

To analyze the phosphoesterase activity of hVps29 in more detail, we generated a model based on the published mVps29 structure [5] of the hVps29 catalytic site containing a binuclear Zn<sup>2+</sup> centre (vide infra) and a bound phosphate (Figure 4). If the substrate phospho-peptide is bound, both metal ions are coordinated by six ligands; metal #1 is coordinated by Asp-8, His-10 (motif I), Asn-39 (motif II), His-117 (motif V), a bridging hydroxide-ion (W1), and O1 of the bound phosphate, whereas metal #2 is coordinated by Asn-39 (motif II), Asp-62 (motif III), His-86 (motif IV), His-115 (motif V), W1 and O2 of the bound phosphate (Figure 4). In this model, the phosphate group is further

positioned by the interaction of the absolutely conserved Arg-14 with the leaving group oxygen (O4) of the phosphorylated peptide.

To study the role of these catalytic site residues in the phosphoesterase reaction, we constructed D8A, N39A, D62A, H86A and H117A mutants as well as a D8A/H86A double mutant of hVps29. GST alone or GST-fusion proteins of hVps26, hVps35, wild-type and mutant hVps29 were produced in *E. coli* and the respective recombinant proteins were separated from their GST tags using thrombin cleavage. Equal amounts of hVps26 and hVps35 proteins were added to samples containing GST alone, wild-type hVps29 or mutant hVps29. Bacterial expression of several catalytic site mutants was less efficient when compared to the wild-type hVps29 protein, as previously reported by Collins et al. [5]. To compare phosphatase activity of different amounts of mutant hVps29 protein with wild-type hVps29 protein, we used a dilution series of the wild-type protein. Recombinant protein expression of each of the mutant constructs was within the range of the dilution series of the wild-type hVps29 protein (Figure 5B). At all concentrations tested, wild-type hVps29 displayed robust *in vitro* phosphatase activity towards the phosphorylated SFHDDpSDEDLLHI substrate after 30 min (Figure 5A).

Each of the catalytic site mutants showed greatly reduced phosphatase activity towards the CI-M6PR serine phosphorylated peptide (Figure 5A), demonstrating that phosphatase activity of the retromer complex can be blocked by introduction of mutations in the catalytic site of hVps29. These findings directly demonstrate that

hVps29 is a phosphatase. Based on the crystal structure of other metallo-phosphatases, we conclude that mutations in Asp-8, Asn-39, Asp-62, His-86 and His-117 disrupt binding of one of the metal ions to the catalytic site of hVps29, leading to ablation of enzymatic activity.

### **Recombinant hVps29 is a zinc-binding protein**

The geometry of the catalytic site of hVps29 best resembles that of the Mn<sup>2+</sup>/Mn<sup>2+</sup> binuclear metal centre of MRE11, a 3'-5' endonuclease from *Pyrococcus furiosus* (PDB code 1II7) [41], so we hypothesized that Vps29 bound metal ions, possibly Mn<sup>2+</sup>, although other metal ions (Cr, Fe, Co, Ni, Cu, and Zn) are known to be present in the active site of metallo-phosphatases as well. To identify metal ions bound to native hVps29, we performed inductively coupled plasma mass spectrometry (ICP-MS) on the hVps29-GST fusion protein and on GST alone (see experimental procedures). Figure 6A shows that the amount of zinc present in samples containing hVps29-GST was much higher than in the samples containing GST alone. This difference was not detected for Mn, Cr, Fe, Co, Ni or Cu (Table 1) or any other element (data not shown). The amount of zinc in samples containing hVps29-GST increased linearly with the amount of hVps29-GST analyzed (Figure 6B), correlating with a relatively constant calculated molar ratio between hVps29-GST and zinc of about 1:0.3. Although a molar ratio of 1:2 is expected, there may be an overestimation of the presence of hVps29-GST in the measured samples, due to the presence of a small amount of GST alone and other contaminating proteins

(Figure 6C). Moreover, it is possible that a fraction of the hVps29-GST fusion proteins, produced in *E. coli*, has an incorrect folding or is not able to acquire zinc molecules co- or post-translationally. Nevertheless, we conclude that recombinant hVps29 is a zinc-binding phosphoesterase. Mutant hVps29 proteins could not be analysed by ICP-MS, due to their reduced expression levels.

### **Inhibition of the phosphatase activity by metal ion chelators**

To investigate the role of the presence of metal ions in the catalytic site of hVps29 on its phosphoesterase activity, we performed phosphatase assays after treatment with several metal ion chelators. Treatment of the recombinantly expressed retromer proteins with a-specific metal ion chelators such as EDTA or EGTA prior to thrombin cleavage, resulted in a 80% reduction of the enzymatic activity of the retromer complex on the SFHDDpSDEDLLHI phosphorylated peptide (Figure 7A). More interestingly, pre-treatment of the recombinantly expressed retromer proteins with the zinc-specific chelator TPEN (N,N,N',N'-tetrakis(2-pyridylmethyl)ethylenediamine) led to a reduction of the phosphatase activity by about 50% (Figure 7A). Re-addition of ZnCl<sub>2</sub> restored the phosphatase activity of the TPEN treated samples to the level of untreated wild-type hVps29 (Figure 7A). Addition of ZnCl<sub>2</sub> without TPEN treatment did not increase the phosphatase activity of the retromer complex on the SFHDDpSDEDLLHI phosphorylated peptide. Protein expression in the phosphatase assay was confirmed by Coomassie blue staining of the

remaining supernatant of the samples used in the assay (Figure 7B). We conclude that hVps29 contains zinc ions which are essential for phosphatase activity of the retromer complex.

### **Functional significance of the Asn-39/Asp-62 switch in hVps29**

As previously discussed, Vps29 is unique among PPP-type metallo-phosphatases because of the presence of Asn-39 (instead of Asp), Asp-62 (instead of Asn) and Phe-63 (instead of a catalytic histidine). To determine the functional significance of the Asn-39/Asp-62 switch for hVps29 phosphatase activity, we introduced the N39D, D62N as well as a N39D/D62N double mutation into pGEX4T3-hVps29 and evaluated the phosphatase activity of these mutants. Recombinant protein expression of each of the mutant constructs was within the range of the dilution series of the wild-type hVps29 protein (Figure 8B). As expected, the N39D mutation had no effect on the phosphatase activity (Figure 8A). Interestingly however, the D62N mutation blocked hVps29 phosphatase activity, which was also seen for the N39D/D62N double mutant. These results indicate that hVps29 Asn-39 can be replaced by an aspartic acid, because both side chains can contribute a metal bridging oxygen at this position. In contrast, Asp-62 cannot be replaced by an asparagine, indicating that both oxygens in the carboxyl group are functionally important in hVps29. This is surprising, as the amino group of asparagine would be ideally suited to bind the phosphate O2 oxygen, an interaction found in all available X-ray structures of ligated metallo-phosphatases.

Since Vps29 lacks the catalytic histidine in motif III, we considered the possibility that Asp-62 might help to replace it. To investigate whether Asp-62 could take the role of the general acid and neutralize the oxy-anion of the leaving group, we performed pKa calculations for the active site residues and found that protonation of Asp-62 is highly unlikely: due to the presence of the metal ions and the strong hydrogen bond between Asn-39 and Asp-62, the predicted pKa of Asp-62 is below zero. The same is true for the histidines close by, which are all involved in metal binding. A more plausible explanation for the importance of Asp-62 is depicted in Figure 4: Asp-62 may help to stabilize a proton on the phosphate O2 atom by forming a hydrogen bond. In the trigonal bipyramidal transition state of the reaction [30], the proton could come sufficiently close to reach the leaving group directly, or alternatively jump via an associated water molecule. Another possible role of Asp-62 might involve protein binding, and its importance is best illustrated by the conservation of a charged residue on this position among several plant and fungal species (Figure S3, supplementary material). Although the complete function of hVps29 Asp-62 remains unclear, its importance for the catalytic activity of hVps29 is clearly demonstrated.

## DISCUSSION

### **hVps29 functions as a phosphoesterase in vitro**

In this study we have characterized the function of the retromer component hVps29. Recently published crystal structures of Vps29 by Wang et

al. and Collins et al. indicate that Vps29 contains a metallo-phosphoesterase fold, but these authors could not experimentally show its phosphoesterase activity [5, 28]. Here, we demonstrate *in vitro* phosphatase activity for the hVps29 containing retromer complex towards a serine phosphorylated peptide SFHDDpSDEDLLHI substrate, containing the acidic-cluster dileucine motif of the CI-M6PR tail. There was no phosphatase activity measured towards the threonine phosphorylated peptide KRpTIRR, which can be dephosphorylated by PP2A (protein phosphatase 2A), demonstrating substrate specificity for the hVps29 containing retromer complex (data not shown).

The discrepancy between the studies with respect to mammalian Vps29 phosphatase activity, may be explained by several differences in the experimental conditions. First, we observed that the phosphatase activity of hVps29 alone was only detectable after prolonged overnight incubation. Moreover, we demonstrated by affinity precipitations that hVps29 interacts with the other retromer subunits, consistent with Collins et al. [5], and that the addition of hVps26 and hVps35 to the reaction mixture greatly enhanced the phosphatase activity. These results indicate that the retromer complex functions as a holo-enzyme complex. Indeed, using hVps26-GST as a bait, we were able to affinity precipitate the hVps29 and hVps35 retromer subunits, which resulted in acquisition of phosphatase activity. The requirement for the other retromer subunits may be due to the involvement of Vps26 and/or Vps35 in (i) substrate recognition [4, 6, 8-10], (ii) contributions of active site residues (vide

infra), and/or (iii) assembly, folding or stability of the active retromer complex [10, 20, 25]. Vps35p is very unstable when either Vps29 or Vps26 is mutated or deleted [10, 20]. Moreover, anti-Vps26 siRNAs treatment of mammalian cell lines does not only lead to depletion of endogenous Vps26, but also to depletion of Vps29 and Vps35 [4, 6], indicating that all retromer subunits must be present to form a stable complex. Second, we avoided any influence of the GST protein on the assembly and activity of the retromer complex. We used recombinant proteins only (i) after the recombinant retromer protein was cleaved from the GST moiety by thrombin or (ii) after replacing the GST moiety by the smaller mycHis-tag.

Third, we demonstrated hVps29 phosphatase activity towards the serine phosphorylated peptide SFHDDpSDEDLLHI substrate. Collins et al. could not detect phosphatase activity of hVps29 towards *p*-nitrophenylphosphate (pNPP)-based substrates and several soluble phosphatidylinositol phosphates [5].

### **hVps29 is a zinc-binding protein**

Apart from the Asn-39/Asp-62 switch, the catalytic site of hVps29 best resembles that of the MRE11 endonuclease which contains a binuclear  $Mn^{2+}$  centre [41]. Collins et al. [5, 28] soaked mVps29 crystals in  $MnSO_4$  and observed that the mVps29 catalytic site can bind bivalent metal ions. However, these studies did not identify the metal ions bound to native Vps29 or the metal ions required for enzymatic activity. ICP-MS analysis revealed that native hVps29 contains  $Zn^{2+}$ . We demonstrated that zinc

binding is involved in the enzymatic activity of hVps29 by performing phosphatase assays with the specific zinc metal chelator TPEN, which reduces the phosphatase activity. Moreover, we demonstrated that addition of  $ZnCl_2$  after TPEN treatment restores the phosphatase activity.

More than 300 enzymes, covering all six classes of enzymes, have been discovered which require zinc ions for their activity [42]. Moreover, zinc is the most common metal used in metallo-enzymes that catalyze hydrolysis or hydration reactions [29]. Importantly, other PPP-type phosphatases, including purple acid phosphatase (PDB code 4KBP) [43], calcineurin (1AUI) [44] and 5'nucleotidase (1USH) [45] also contain  $Zn^{2+}$  ions in their catalytic site.

### **Implications for the catalytic mechanism**

Even though we were able to demonstrate phosphatase activity for the retromer complex, many questions regarding the enzymatic reaction remain. First, the identity of the nucleophile that attacks the phosphate is unclear. The active site of metallo-phosphoesterases contains water molecules, one of which is invariably involved in the coordination of both metal ions in a  $\mu$ -hydroxo bridge (W1) (Figure 4). Frequently, a second water molecule (W2) is detected bound to metal #1. Which of these water molecules acts as the nucleophile during catalysis is a question of debate [46]. In general, the pKa of W1 is sufficiently low to be deprotonated and to become a hydroxide ion. Opposite of the leaving group, W1 is also in an ideal position for in-line attack of the phosphorus atom. However, as W1 binding to both metal ions reduces its nucleophilicity, it has been suggested that metal

#1-bound W2 is the nucleophile that attacks the phospho-ester bond [40]. However, this mechanism was proposed for purple acid phosphatase coordinating two different metal ions,  $Zn^{2+}$  and  $Fe^{3+}$  [43]. Binding of trivalent  $Fe^{3+}$  to W2 can lower the pKa of W2 sufficiently such that W2 exists as a hydroxide ion at physiological pH. In contrast, bivalent  $Zn^{2+}$  ions cannot lower the pKa of terminally ligated water molecule sufficiently to create a hydroxide ion by itself at physiological pH [47]. In that case, a general base may be required to further lower the pKa of W2. Although we cannot exclude that W2 (if existing) is the nucleophilic hydroxide molecule, we favour the hypothesis that the hydroxide ion W1 is the one that is involved in the nucleophilic attack, as discussed in detail by Swingle et al. [30].

The second question that remains concerns the identity of the proton donor that protonates the oxy-anion of the leaving group. Unlike most other eukaryotic PPP-type metallo-phosphatases, Vps29 lacks a catalytic histidine in motif III. Building on their negative results with respect to Vps29 phosphatase activity, Collins et al. [5] suggested that another cofactor (such as Vps26 or Vps35) might contribute a catalytic histidine to the Vps29 active site. Based on current (draft) whole genome sequencing programs, both Vps26 and Vps35 retromer proteins contain histidine residues that are nearly absolutely conserved among all eukaryotes and could be candidates for the delivery of the missing histidine (data not shown). However, the low but measurable *in vitro* phosphatase activity of hVps29 in the absence of hVps26 and hVps35 seems inconsistent with such a model. In addition,

molecular modelling suggests that there is very little space to insert a histidine in the gap that is created by the outward movement of Phe-63 that occurs upon metal binding (E. Krieger, data not shown). It should be noted that we cannot exclude the possibility that conformational changes occur in the Vps29 catalytic site upon assembly of the holo-retromer complex. Importantly, despite lacking a catalytic histidine in motif III, the archaeal protein MJ0936 is also an active metallo-phosphoesterase [48], indicating that a catalytic histidine is not absolutely required for phosphoesterase activity. Yet another possibility that needs to be considered is that there is no specific proton donor for the leaving group, and that the leaving group slowly retrieves a proton from bulk water. Finally, it is important to realise that the pKa calculations must be interpreted with caution: they were performed on hVps29 alone, in the presence of the binuclear  $Zn^{2+}$  centre and in the presence or absence of bound tri-anionic phosphate, even though it is clear that the enzymatic activity of hVps29 is greatly enhanced when bound to hVps26 and hVps35. Given that mVps35 binds close to the mVps29 active site [5], it is conceivable that the immediate environment of the Vps29 active site, i.e. the charge distribution and thus the predicted pKa values, is changed upon incorporation of Vps29 in the holo-retromer complex. Crystallization of the holo-retromer complex will probably be necessary to answer some of these questions.

A third question that remains concerns the evolutionary conservation of Vps29 enzymatic function. Although metal coordinating catalytic site residues of Vps29 are highly conserved in

most metazoans, there are multiple substitutions in those residues among pseudo-coelomate nematodes, various fungal and protozoan species (Figure S3, supplementary material). It remains to be demonstrated whether the retromer complex displays phosphatase activity in yeast and other species or whether there may be functional differences in the retromer complex among species.

### **Trafficking of the CI-M6PR depends on the phosphorylation status of the receptor**

We demonstrate that the retromer component hVps29 interacts with hVps26 and hVps35 retromer subunits and functions *in vitro* as a phosphoesterase for a phosphopeptide based on the sequence of the CI-M6PR tail. A working model for the *in vivo* role of hVps29-mediated dephosphorylation of the acidic-cluster dileucine motif of the CI-M6PR is presented in Figure 9. After binding to mannose 6-phosphate-tagged lysosomal hydrolases in the TGN, the phosphorylation of Ser-2492 within the acidic-cluster dileucine motif acts as a sorting signal for anterograde transport by binding to GGA1 and GGA3 [23]. The GGA proteins will transport the CI-M6PR by clathrin coated pits to the endosome. In the endosome the CI-M6PR will dissociate from its ligand, which is subsequently transported to the lysosome. On the endosome, the CI-M6PR co-localizes with the retromer complex [4, 6]. It is tempting to speculate that after binding of mammalian Vps35 to the CI-M6PR in the endosome, Vps29 will dephosphorylate the receptor. Dephosphorylation of this trafficking motif might be the trigger for

the CI-M6PR to recycle back to the TGN to carry out additional rounds of enzyme delivery. This model remains to be confirmed by *in vivo* data of dephosphorylation of the CI-M6PR by hVps29. In addition, the exact role of dephosphorylation of the CI-M6PR on the transport of the receptor remains to be investigated. Other proteins that have been implicated in endosome-to-Golgi retrieval of the cycling TGN proteins are TIP47 (tail-interacting protein of 47 kD) [49] and PACS-1 (phosphofurin cluster sorting protein-1) [50]. However, neither of these proteins is evolutionary conserved among eukaryotes and therefore may not be fundamental for the eukaryote retrograde endosome-to-TGN vesicular transport pathway.

In addition, it is interesting to note that Vps29 may function as a phosphoesterase for other substrates as well. Mutational analysis of the serine phosphorylated peptide SFHDDpSDEDLLHI could reveal a minimal sequence motif required for Vps29 dependent dephosphorylation. In yeast, Vps35 does not only bind the Vps10p receptor but also A-ALP (alkaline phosphatase) [11, 51], so its cytosolic tail DPAP A (dipeptidyl aminopeptidase A) is also an interesting candidate for dephosphorylation by Vps29. Since mammalian Vps35 is known to interact with the CI-M6PR [4, 6, 9], it is tempting to speculate that Vps29 may be involved in dephosphorylation of other acidic-cluster dileucine motifs as well, many of which are regulated by serine phosphorylation like the CD-M6PR and furin [52, 53].



The authors thank Prof. E.J.J. van Zoelen, Dr. S.M. Jansen and Dr. E.J. Reijerse for helpful discussions and E.M. Bilkerdijk and M.J.C.M. Koopmans for construction of several hVps29 mutants. Financial support for this project was provided by research grants from Zon-MW (908-02-047).

## REFERENCES

- 1 Bankaitis, V. A., Johnson, L. M. and Emr, S. D. (1986) Isolation of yeast mutants defective in protein targeting to the vacuole. *Proc Natl Acad Sci U S A* **83**, 9075-9079
- 2 Robinson, J. S., Klionsky, D. J., Banta, L. M. and Emr, S. D. (1988) Protein sorting in *Saccharomyces cerevisiae*: isolation of mutants defective in the delivery and processing of multiple vacuolar hydrolases. *Mol Cell Biol* **8**, 4936-4948
- 3 Rothman, J. H. and Stevens, T. H. (1986) Protein sorting in yeast: mutants defective in vacuole biogenesis mislocalize vacuolar proteins into the late secretory pathway. *Cell* **47**, 1041-1051
- 4 Arighi, C. N., Hartnell, L. M., Aguilar, R. C., Haft, C. R. and Bonifacino, J. S. (2004) Role of the mammalian retromer in sorting of the cation-independent mannose 6-phosphate receptor. *J Cell Biol* **165**, 123-133
- 5 Collins, B. M., Skinner, C. F., Watson, P. J., Seaman, M. N. and Owen, D. J. (2005) Vps29 has a phosphoesterase fold that acts as a protein interaction scaffold for retromer assembly. *Nat Struct Mol Biol*
- 6 Seaman, M. N. (2004) Cargo-selective endosomal sorting for retrieval to the Golgi requires retromer. *J Cell Biol* **165**, 111-122
- 7 Seaman, M. N., McCaffery, J. M. and Emr, S. D. (1998) A membrane coat complex essential for endosome-to-Golgi retrograde transport in yeast. *J Cell Biol* **142**, 665-681
- 8 Cereghino, J. L., Marcusson, E. G. and Emr, S. D. (1995) The cytoplasmic tail domain of the vacuolar protein sorting receptor Vps10p and a subset of VPS gene products regulate receptor stability, function, and localization. *Mol Biol Cell* **6**, 1089-1102
- 9 Cooper, A. A. and Stevens, T. H. (1996) Vps10p cycles between the late-Golgi and prevacuolar compartments in its function as the sorting receptor for multiple yeast vacuolar hydrolases. *J Cell Biol* **133**, 529-541

- 10 Marcusson, E. G., Horazdovsky, B. F., Cereghino, J. L., Gharakhanian, E. and Emr, S. D. (1994) The sorting receptor for yeast vacuolar carboxypeptidase Y is encoded by the VPS10 gene. *Cell* **77**, 579-586
- 11 Nothwehr, S. F., Ha, S. A. and Bruinsma, P. (2000) Sorting of yeast membrane proteins into an endosome-to-Golgi pathway involves direct interaction of their cytosolic domains with Vps35p. *J Cell Biol* **151**, 297-310
- 12 Kornfeld, S. (1992) Structure and function of the mannose 6-phosphate/insulinlike growth factor II receptors. *Annu Rev Biochem* **61**, 307-330
- 13 Meresse, S. and Hoflack, B. (1993) Phosphorylation of the cation-independent mannose 6-phosphate receptor is closely associated with its exit from the trans-Golgi network. *J Cell Biol* **120**, 67-75
- 14 Boman, A. L., Zhang, C., Zhu, X. and Kahn, R. A. (2000) A family of ADP-ribosylation factor effectors that can alter membrane transport through the trans-Golgi. *Mol Biol Cell* **11**, 1241-1255
- 15 Dell'Angelica, E. C., Puertollano, R., Mullins, C., Aguilar, R. C., Vargas, J. D., Hartnell, L. M. and Bonifacino, J. S. (2000) GGAs: a family of ADP ribosylation factor-binding proteins related to adaptors and associated with the Golgi complex. *J Cell Biol* **149**, 81-94
- 16 Hirst, J., Lui, W. W., Bright, N. A., Totty, N., Seaman, M. N. and Robinson, M. S. (2000) A family of proteins with gamma-adaptin and VHS domains that facilitate trafficking between the trans-Golgi network and the vacuole/lysosome. *J Cell Biol* **149**, 67-80
- 17 Poussu, A., Lohi, O. and Lehto, V. P. (2000) Vear, a novel Golgi-associated protein with VHS and gamma-adaptin "ear" domains. *J Biol Chem* **275**, 7176-7183
- 18 Takatsu, H., Yoshino, K. and Nakayama, K. (2000) Adaptor gamma ear homology domain conserved in gamma-adaptin and GGA proteins that interact with gamma-synergin. *Biochem Biophys Res Commun* **271**, 719-725

- 19 Puertollano, R., Randazzo, P. A., Presley, J. F., Hartnell, L. M. and Bonifacino, J. S. (2001) The GGAs promote ARF-dependent recruitment of clathrin to the TGN. *Cell* **105**, 93-102
- 20 Takatsu, H., Katoh, Y., Shiba, Y. and Nakayama, K. (2001) Golgi-localizing, gamma-adaptin ear homology domain, ADP-ribosylation factor-binding (GGA) proteins interact with acidic dileucine sequences within the cytoplasmic domains of sorting receptors through their Vps27p/Hrs/STAM (VHS) domains. *J Biol Chem* **276**, 28541-28545
- 21 Zhu, Y., Doray, B., Poussu, A., Lehto, V. P. and Kornfeld, S. (2001) Binding of GGA2 to the lysosomal enzyme sorting motif of the mannose 6-phosphate receptor. *Science* **292**, 1716-1718
- 22 Doray, B., Bruns, K., Ghosh, P. and Kornfeld, S. (2002) Interaction of the cation-dependent mannose 6-phosphate receptor with GGA proteins. *J Biol Chem* **277**, 18477-18482
- 23 Kato, Y., Misra, S., Puertollano, R., Hurley, J. H. and Bonifacino, J. S. (2002) Phosphoregulation of sorting signal-VHS domain interactions by a direct electrostatic mechanism. *Nat Struct Biol* **9**, 532-536
- 24 Haft, C. R., de la Luz Sierra, M., Bafford, R., Lesniak, M. A., Barr, V. A. and Taylor, S. I. (2000) Human orthologs of yeast vacuolar protein sorting proteins Vps26, 29, and 35: assembly into multimeric complexes. *Mol Biol Cell* **11**, 4105-4116
- 25 Reddy, J. V. and Seaman, M. N. (2001) Vps26p, a component of retromer, directs the interactions of Vps35p in endosome-to-Golgi retrieval. *Mol Biol Cell* **12**, 3242-3256
- 26 Horazdovsky, B. F., Davies, B. A., Seaman, M. N., McLaughlin, S. A., Yoon, S. and Emr, S. D. (1997) A sorting nexin-1 homologue, Vps5p, forms a complex with Vps17p and is required for recycling the vacuolar protein-sorting receptor. *Mol Biol Cell* **8**, 1529-1541
- 27 Seaman, M. N. and Williams, H. P. (2002) Identification of the functional domains of yeast sorting nexins Vps5p and Vps17p. *Mol Biol Cell* **13**, 2826-2840

- 28 Wang, D., Guo, M., Liang, Z., Fan, J., Zhu, Z., Zang, J., Zhu, Z., Li, X., Teng, M., Niu, L., Dong, Y. and Liu, P. (2005) Crystal structure of human vacuolar protein sorting protein 29 reveals a phosphodiesterase/nuclease-like fold and two protein-protein interaction sites. *J Biol Chem*
- 29 Christianson, D. W. and Cox, J. D. (1999) Catalysis by metal-activated hydroxide in zinc and manganese metalloenzymes. *Annu Rev Biochem* **68**, 33-57
- 30 Swingle, M. R., Honkanen, R. E. and Ciszak, E. M. (2004) Structural basis for the catalytic activity of human serine/threonine protein phosphatase-5. *J Biol Chem* **279**, 33992-33999
- 31 Jung, J. and Lee, B. (2000) Protein structure alignment using environmental profiles. *Protein Eng* **13**, 535-543
- 32 Krieger, E., Darden, T., Nabuurs, S. B., Finkelstein, A. and Vriend, G. (2004) Making optimal use of empirical energy functions: force-field parameterization in crystal space. *Proteins* **57**, 678-683
- 33 Nielsen, J. E. and Vriend, G. (2001) Optimizing the hydrogen-bond network in Poisson-Boltzmann equation-based pK(a) calculations. *Proteins* **43**, 403-412
- 34 Nicholls, A. and Honig, B. (1991) A rapid finite difference algorithm, utilizing successive over-relaxation to solve the Poisson-Boltzmann equation. *J Comp Chem* **12**, 435-445
- 35 Jorgensen, W. L. and Tirado-Rives, J. (1988) The OPLS potential functions for proteins: energy minimizations for crystals for cyclic peptides and crambin. *J Am Chem Soc* **110**, 1657-1666
- 36 Kennelly, P. J. (2003) Archaeal protein kinases and protein phosphatases: insights from genomics and biochemistry. *Biochem J* **370**, 373-389
- 37 Barford, D., Das, A. K. and Egloff, M. P. (1998) The structure and mechanism of protein phosphatases: insights into catalysis and regulation. *Annu Rev Biophys Biomol Struct* **27**, 133-164

- 38 Koonin, E. V., Mushegian, A. R., Tatusov, R. L., Altschul, S. F., Bryant, S. H., Bork, P. and Valencia, A. (1994) Eukaryotic translation elongation factor 1 gamma contains a glutathione transferase domain--study of a diverse, ancient protein superfamily using motif search and structural modeling. *Protein Sci* **3**, 2045-2054
- 39 Zhuo, S., Clemens, J. C., Stone, R. L. and Dixon, J. E. (1994) Mutational analysis of a Ser/Thr phosphatase. Identification of residues important in phosphoesterase substrate binding and catalysis. *J Biol Chem* **269**, 26234-26238
- 40 Klabunde, T., Strater, N., Frohlich, R., Witzel, H. and Krebs, B. (1996) Mechanism of Fe(III)-Zn(II) purple acid phosphatase based on crystal structures. *J Mol Biol* **259**, 737-748
- 41 Hopfner, K. P., Karcher, A., Craig, L., Woo, T. T., Carney, J. P. and Tainer, J. A. (2001) Structural biochemistry and interaction architecture of the DNA double-strand break repair Mre11 nuclease and Rad50-ATPase. *Cell* **105**, 473-485
- 42 McCall, K. A., Huang, C. and Fierke, C. A. (2000) Function and mechanism of zinc metalloenzymes. *J Nutr* **130**, 1437S-1446S
- 43 Strater, N., Klabunde, T., Tucker, P., Witzel, H. and Krebs, B. (1995) Crystal structure of a purple acid phosphatase containing a dinuclear Fe(III)-Zn(II) active site. *Science* **268**, 1489-1492
- 44 Kissinger, C. R., Parge, H. E., Knighton, D. R., Lewis, C. T., Pelletier, L. A., Tempczyk, A., Kalish, V. J., Tucker, K. D., Showalter, R. E., Moomaw, E. W. and et al. (1995) Crystal structures of human calcineurin and the human FKBP12-FK506-calcineurin complex. *Nature* **378**, 641-644
- 45 Knofel, T. and Strater, N. (1999) X-ray structure of the Escherichia coli periplasmic 5'-nucleotidase containing a dimetal catalytic site. *Nat Struct Biol* **6**, 448-453
- 46 Lindqvist, Y., Johansson, E., Kaija, H., Vihko, P. and Schneider, G. (1999) Three-dimensional structure of a mammalian purple acid phosphatase at 2.2 Å resolution with a  $\mu$ -(hydr)oxo bridged di-iron center. *J Mol Biol* **291**, 135-147

- 47 Baes, C. F., Mesmer, R.E. (1976) *The Hydrolysis of Cations*. Wiley-Interscience, New York, 219-237
- 48 Chen, S., Yakunin, A. F., Kuznetsova, E., Busso, D., Pufan, R., Proudfoot, M., Kim, R. and Kim, S. H. (2004) Structural and functional characterization of a novel phosphodiesterase from *Methanococcus jannaschii*. *J Biol Chem* **279**, 31854-31862
- 49 Diaz, E. and Pfeffer, S. R. (1998) TIP47: a cargo selection device for mannose 6-phosphate receptor trafficking. *Cell* **93**, 433-443
- 50 Wan, L., Molloy, S. S., Thomas, L., Liu, G., Xiang, Y., Rybak, S. L. and Thomas, G. (1998) PACS-1 defines a novel gene family of cytosolic sorting proteins required for trans-Golgi network localization. *Cell* **94**, 205-216
- 51 Nothwehr, S. F., Bruinsma, P. and Strawn, L. A. (1999) Distinct domains within Vps35p mediate the retrieval of two different cargo proteins from the yeast prevacuolar/endosomal compartment. *Mol Biol Cell* **10**, 875-890
- 52 Breuer, P., Korner, C., Boker, C., Herzog, A., Pohlmann, R. and Braulke, T. (1997) Serine phosphorylation site of the 46-kDa mannose 6-phosphate receptor is required for transport to the plasma membrane in Madin-Darby canine kidney and mouse fibroblast cells. *Mol Biol Cell* **8**, 567-576
- 53 Jones, B. G., Thomas, L., Molloy, S. S., Thulin, C. D., Fry, M. D., Walsh, K. A. and Thomas, G. (1995) Intracellular trafficking of furin is modulated by the phosphorylation state of a casein kinase II site in its cytoplasmic tail. *Embo J* **14**, 5869-5883

## FIGURE LEGENDS

### Table 1 Detected amounts of metal ions in hVps29-GST by ICP-MS

Samples of recombinantly expressed hVps29-GST fusion protein and GST alone with an increasing amount of molecules were analysed by ICP-MS. Depicted are the amounts in parts per billion (ppb) of those metal ions which were the best candidates for binding to hVps29-GST.

### Figure 1 Interaction of hVps29 with hVps26 and hVps35 *in vitro*

(A) GST fusion proteins were used as an affinity matrix for hVps26, hVps29 and hVps35 YFP fusion proteins present in the lysates of transiently transfected NIH3T3 cells. Affinity precipitated proteins were visualised by Western blotting with anti-GFP antibodies. (v: vector; 26: Vps26; 29: Vps29 and 35: Vps35) (B) Western blot of whole cell lysate samples of NIH3T3 cells transfected with the YFP fusion constructs, detected with anti-GFP antibodies. (C) Coomassie staining of the GST-fusion constructs used for the pull down assay.

### Figure 2 Phosphatase activity of hVps29 on a CI-M6PR phosphopeptide

(A) Coomassie blue staining of recombinantly expressed GST fusion proteins of vector (26 kDa), hVps26 (36 kDa), hVps29 (20 kDa) and hVps35 (87 kDa) before and after thrombin cleavage. (B) Detected amounts of free phosphate in an *in vitro* phosphatase assay on the SFHDDpSDEDLLHI phosphopeptide using recombinantly expressed vector, hVps26, hVps29, hVps35 or a mixture of these three proteins. Levels of free phosphate were determined after 30 min and 16 hrs of incubation. (C) Coomassie blue staining of the remaining supernatant of the protein samples used for the *in vitro* phosphatase assay.

### Figure 3 Phosphatase assay on affinity precipitated retromer complex

(A) Western blot with anti-c-Myc antibody. Lane 1-3, expression of purified mycHis constructs following metal chelation affinity chromatography with Ni-NTA beads. Lane 4-5, hVps26-GST affinity precipitation following incubation with mycHis vector or with purified mycHis hVps29 and hVps35 proteins. (v: vector; 29: Vps29 and 35: Vps35) (B) Detected amounts of free phosphate in an *in vitro* phosphatase assay on the SFHDDpSDEDLLHI phosphopeptide using GST vector (bar 1), an affinity precipitation of Vps26-GST containing Vps29 and Vps35 mycHis fusion proteins (bar 2) or as a positive control, a mixture of hVps26, hVps29, hVps35 proteins (bar 3), as used in Figure 2. Levels of free phosphate were determined after 30 min of incubation. (C) Coomassie blue staining of the remaining supernatant of the protein samples used for the *in vitro* phosphatase assay.



**Figure 4 Molecular model of the hVps29 active site**

The catalytic site of hVps29 showing two Zn<sup>2+</sup> ions, the coordinating amino acid side chains and a bound phosphate. The hydroxide ion bridging the two metal ions is labelled 'W1' and hydrogen-bonded to the backbone oxygen of His-115. Only polar hydrogens are shown. The serine residue of the substrate peptide has been omitted, but should be connected to the now protonated phosphate oxygen. Image was created with YASARA ([www.yasara.org](http://www.yasara.org)).

**Figure 5 Inhibition of the phosphatase activity of hVps29 by catalytic site mutants**

(A) Detected amounts of free phosphate in an *in vitro* phosphatase assay on the SFHDDpSDEDLLHI phosphopeptide using recombinantly expressed hVps26 and hVps35 in combination with vector, wild-type hVps29 in increasing concentrations or hVps29 mutants D8A, N39A, D62A, H86A, H117A or D8A/H86A. Levels of free phosphate were determined after 30 min of incubation. (B) Coomassie blue staining of the remaining supernatant of the protein samples used for the *in vitro* phosphatase assay.

**Figure 6 Detected amounts of zinc ions in hVps29-GST by ICP-MS**

(A) Binding of zinc ions in ppb to increasing amounts of recombinantly expressed hVps29-GST fusion protein or GST alone. (B) Linear increase of the amount of zinc by increasing amounts of recombinantly expressed hVps29-GST fusion protein corrected for binding to GST alone. The slope of the line indicates the molar ratio of hVps29-GST: zinc. (C) Coomassie blue staining of a small amount of the recombinantly expressed proteins used in the ICP-MS analysis. The protein amount was measured by photo-spectrometric analysis (data not shown), but also by comparison with BSA levels.

**Figure 7 Inhibition of the phosphatase activity of hVps29 by metal ion chelators**

(A) Detected amounts of free phosphate in an *in vitro* phosphatase assay on the SFHDDpSDEDLLHI phosphopeptide using recombinantly expressed hVps26 and hVps35 in combination with vector as a control or wild-type hVps29. Samples were treated with 5 mM of the indicated metal ion chelators prior to thrombin cleavage. When indicated, ZnCl<sub>2</sub> was added to the reaction mixture to a final concentration of 1 mM. Levels of free phosphate were determined after 30 min of incubation. (B) Coomassie blue staining of the remaining supernatant of the protein samples used for the *in vitro* phosphatase assay.

**Figure 8 Effect of the Asn-39/Asp-62 pair on the phosphatase activity**

(A) Detected amounts of free phosphate in an *in vitro* phosphatase assay on the SFHDDpSDEDLLHI phosphopeptide using recombinantly expressed hVps26 and hVps35 in combination with vector, wild-type hVps29 in increasing concentrations, hVps29 mutants N39A, N39D, D62A, D62N and N39D/D62N. Levels of free phosphate were determined after 30 min of incubation. (B) Coomassie

blue staining of the remaining supernatant of the protein samples used for the *in vitro* phosphatase assay.

**Figure 9 Model of phosphate dependent transport of the CI-M6PR**

The CI-M6PR binds cathepsin D in the TGN. Binding of GGAs to the phosphorylated CI-M6PR causes the transport of the ligand-receptor complex to the endosome. In the endosome, the ligand dissociates from the receptor and after binding to Vps35, Vps29 is able to dephosphorylate the receptor. The retromer recycles the CI-M6PR to the TGN.

Table 1

		GST protein molecules x 10 <sup>15</sup>			
		2.58	6.45	12.9	19.4
		metal ions in ppb			
Mg	GST	0.757	0.058	0.436	0.681
	Vps29	0.978	2.372	0.034	1.125
Ca	GST	111.7	62.8	81.7	122.1
	Vps29	116.2	217.4	51.1	77.5
Cr	GST	0.337	0.212	0	0.549
	Vps29	0	0.222	0	0.164
Fe	GST	20.56	0	0	102.8
	Vps29	0	0	0	0.9
Mn	GST	0.212	0	0	1.268
	Vps29	0	0	0	0.02
Ni	GST	0.499	0.134	0	1.548
	Vps29	0	0.183	0	0.002
Co	GST	0.036	0.006	0.006	0.021
	Vps29	0.006	0.013	0.025	0.036
Cu	GST	0.515	0	0	0.346
	Vps29	0.062	1.458	0.181	0.656
Zn	GST	3.229	2.682	1.933	0.886
	Vps29	25.08	52.58	84.08	135.3

# Figure 1

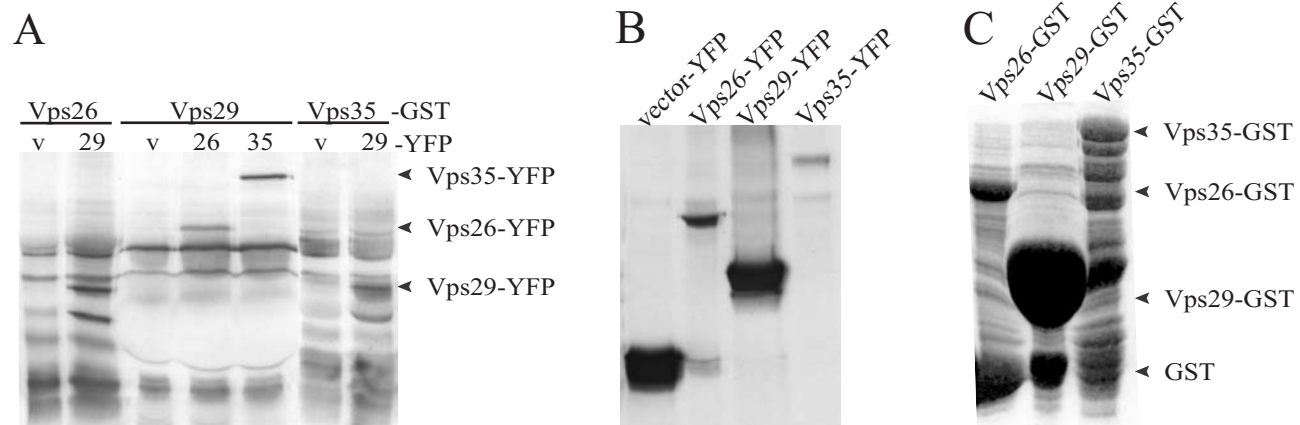


## Figure 2

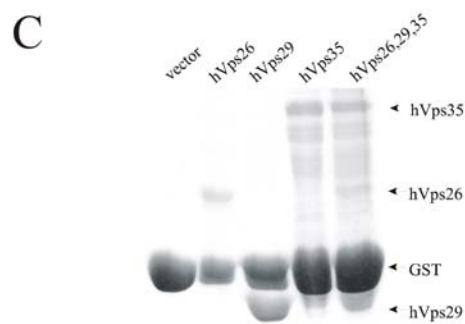
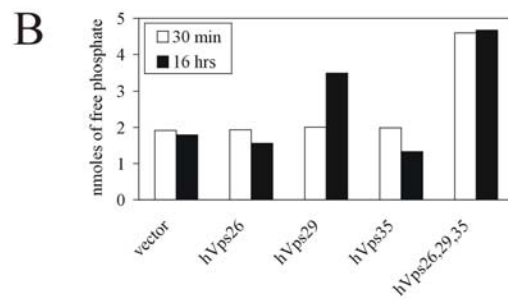
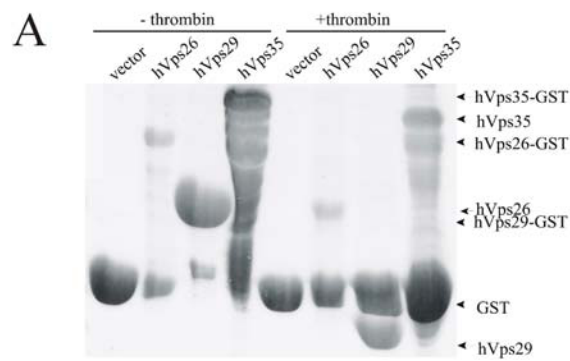


# Figure 3

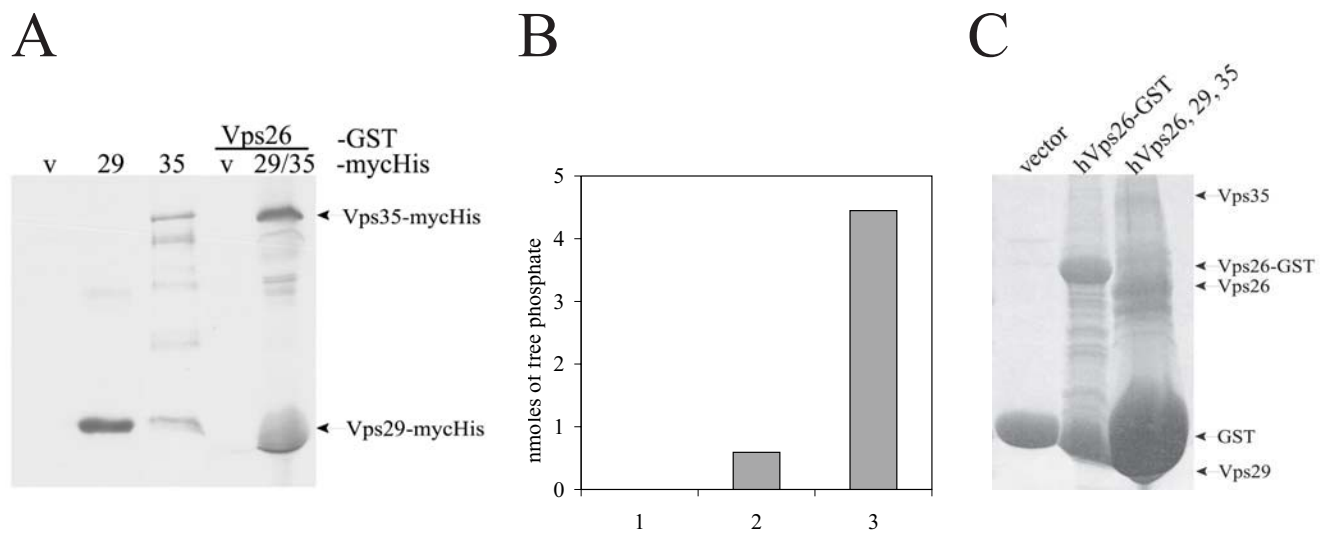


**Figure 4**

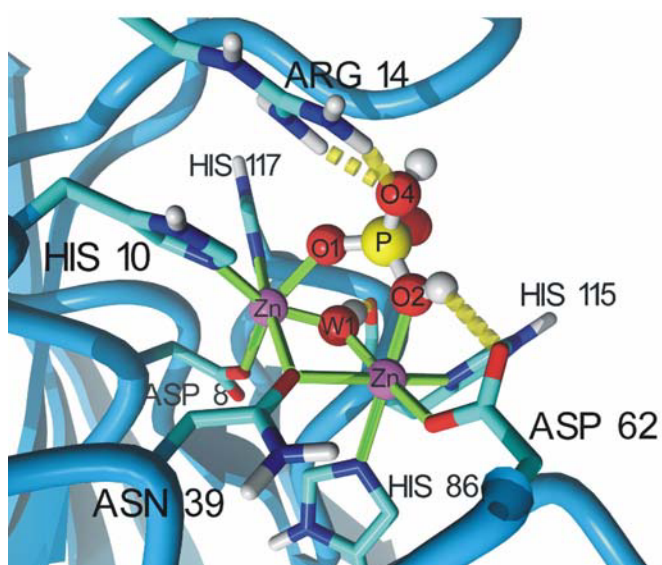


**Figure 5**

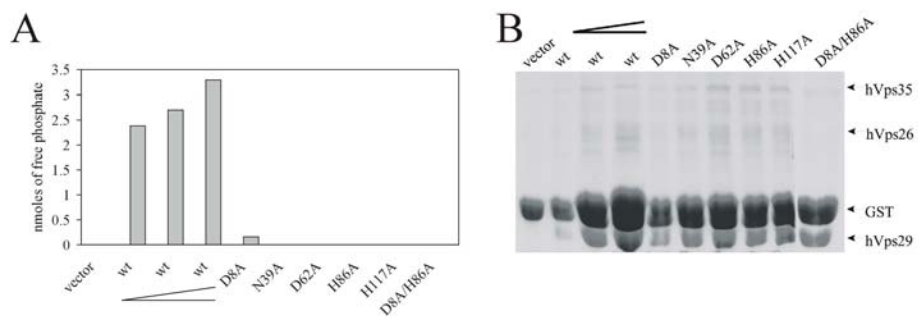




**Figure 6**

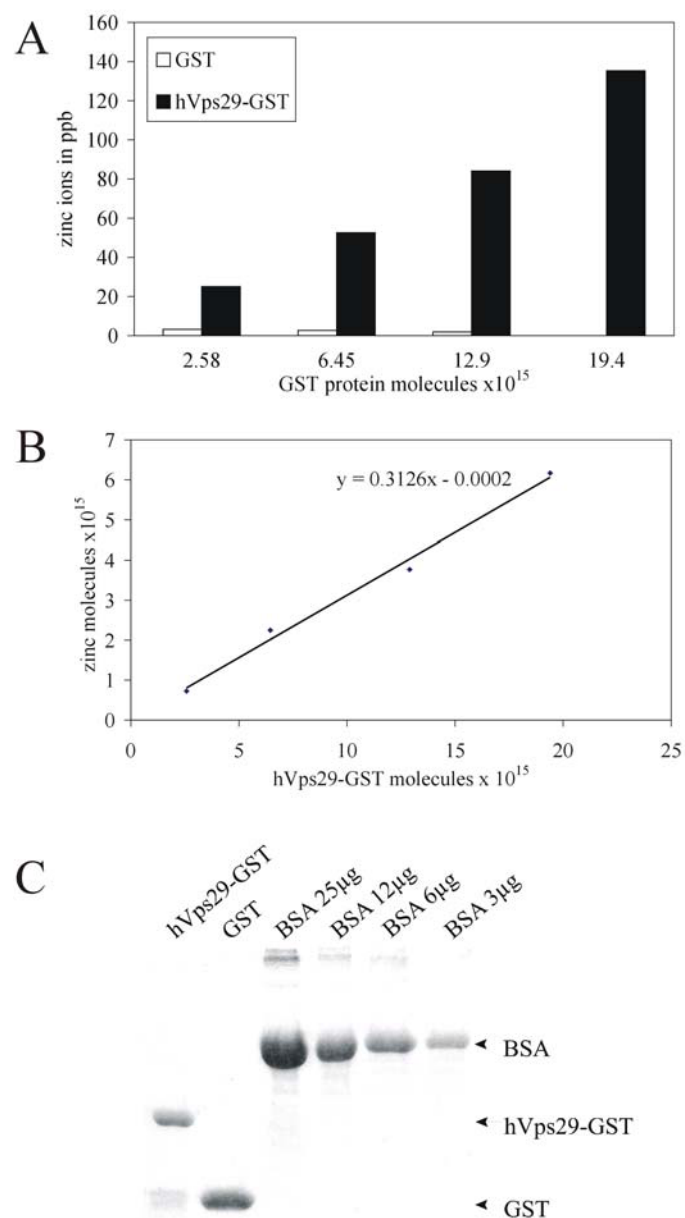


**Figure 7**

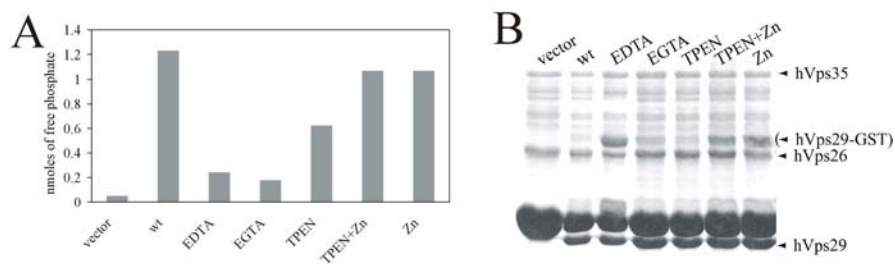


**Figure 8**

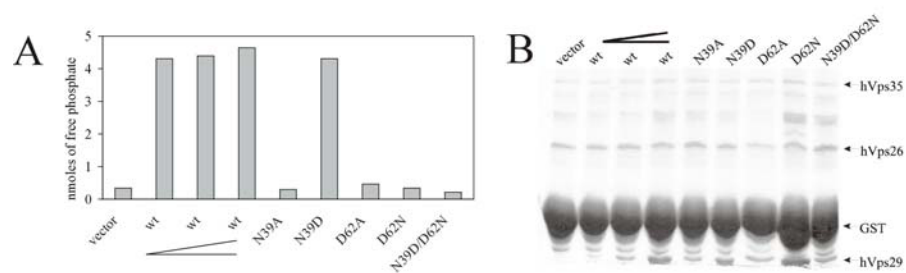


Figure 9

